A microstructure-composition map of a ternary liquid/liquid/particle system with partially-wetting particles†

Junyi Yang, [ID] [a] David Roell,[b] Martin Echavarria[a] and Sachin S. Velankar [ID] *[ac]

We examine the effect of composition on the morphology of a ternary mixture comprising two molten polymeric liquid phases (polyisobutylene and polyethylene oxide) and micron-scale spherical silica particles. The silica particles were treated with silanes to make them partially wetted by both polymers. Particle loadings up to 30 vol% are examined while varying the fluid phase ratios across a wide range. Numerous effects of particle addition are catalogued, stabilization of Pickering emulsions and of interfacially-jammed co-continuous microstructures, meniscus-bridging of particles, particle-induced coalescence of the dispersed phase, and significant shifts in the phase inversion composition. Many of the effects are asymmetric, for example particle-induced coalescence is more severe and drop sizes are larger when polyisobutylene is the continuous phase, and particles promote phase continuity of the polyethylene oxide. These asymmetries are likely attributable to a slight preferential wettability of the particles towards the polyethylene oxide. A state map is constructed which classifies the various microstructures within a triangular composition diagram. Comparisons are made between this diagram *vs.* a previous one constructed for the case when particles are fully-wetted by polyethylene oxide.

1. Introduction

Ternary mixtures of liquid/fluid/particles show a wide diversity of microstructures, many of which have been reviewed in two recent articles.[1,2] Much of the structural diversity is attributable to the capillary-induced interaction between particles: pairwise attraction through capillary bridging,[3–6] many-body cohesion through capillary clustering,[5] interfacial assembly of particles[7–9] or particle bridging of drops.[10,11] Even a single ternary system can display several different morphologies depending on its composition. A recent article by one of us suggested that given a pair of fluids and a particulate species, mixtures of various composition can be conveniently classified within a triangular compositional diagram, with different regions of composition space corresponding to distinct morphologies.[2] Previous papers[5,12–16] from our group examined the morphology of ternary blends composed of two immiscible polymers (polyethylene oxide, PEO and polyisobutylene, PIB), and polydisperse silica particles that have a strong affinity for the PEO. Five types of morphology were

identified at various compositions of this single system: (1) pendular/funicular network, (2) capillary aggregates network, (3) particle-filled drops, (4) co-continuous and (5) drops-in-suspension. Schematics of these structures, and their location on a triangular morphological map were presented previously[14,16] and are reproduced in Fig. S1 (ESI†). To our knowledge, this morphological map covers widest composition range for any single liquid/fluid/particle system in the literature.

That research[5,12–16] was all conducted with particles that are fully-wetted by one of the two phases (PEO). This immediately raises the question of how the morphological map would change if the particles were partially-wetted by both phases. Most studies of partial wettability in three-phase liquid/liquid/particle systems have been conducted in oil/water/particle mixtures. The most heavily-studied example is of Ramsden–Pickering emulsions[17–19] in which the particles act somewhat like surfactants by adsorbing at the liquid–fluid interface, hence inhibiting drop coalescence and stabilizing the emulsion. There have also been studies of bridged Pickering emulsions, *i.e.* emulsions in which a monolayer of particles at the interface bridges together two droplets and hence assembles the droplets into volume-spanning networks.[10,11,20] The presence of interfacially active particles can also stabilize bicontinuous structures through arrested spinodal decomposition of the fluids.[8,9,21] Finally, with partially-wetting particles, particle aggregation into space-spanning networks has also been noted in oil/water/particle mixtures.[22]

[a] *Department of Chemical and Petroleum Engineering, University of Pittsburgh, Pittsburgh, PA 15260, USA*

[b] *Department of Plastics Engineering, Penn State Erie, Erie, PA 16563, USA*

[c] *Department. of Mechanical Engineering and Materials Science, University of Pittsburgh, Pittsburgh, PA 15260, USA. E-mail: velankar@pitt.edu*

† Electronic supplementary information (ESI) available. See DOI: 10.1039/c7sm01571b

Paper

Soft Matter

Going beyond small molecule systems, similar microstructures and phenomena have been noted in ternary systems in which the two fluids are molten polymers.[2,23]

Despite the research cited in the previous paragraph, a comprehensive mapping of the morphology-composition space has never been conducted for situations where the particles are partially-wetted by both liquid phases. Most significantly, the effect of particles at higher loadings remain very poorly understood. Virtually all of the research cited in the previous paragraph has been conducted at relatively low particle loadings, typically lower than 10% by volume, often lower than 2%. There are a few articles at particle loadings exceeding 15 vol%[4,10,14,16,22,24,25] but many of these do not cover a wide range of fluid phase fractions. The goal of this paper therefore is to construct a comprehensive morphological map that is completely analogous to Fig. S1 (ESI†), but with the key difference that the particles are partially wetted by both liquid phases.

It must be emphasized that the only difference between this work and the research leading to Fig. S1 (ESI†) is that the particles in this work are hydrophobically-modified. Other than that, all the remaining materials and methods are identical. Thus, the final morphological maps (Fig. 6) in this paper, and Fig. S1 (ESI†), constitute two different slices of the composition-wettability prism of a single experimental system. Conceptually, such morphological classification within a prism resembles oil–water–surfactant equilibrium phase diagrams,[26,27] except that the current mixtures are far from equilibrium.

We proceed in the following sequence. Section 2 describes the materials and methods, including the method used for hydrophobic modification of particles. Section 3 first verifies that the modified particles are indeed partially-wetted by both fluid phases, and then examines the effect of particles on the morphology at various fluid ratios and particle loadings. Section 4 discusses the results, most importantly, the effect of particles on phase inversion and co-continuity, and interfacial jamming.

2. Experimental

2.1 Materials

Polyisobutylene (PIB, $\rho \approx 0.908$ g mL^{-1}, $M_w \approx 2200$ g mol^{-1}) polyethyleneoxide (PEO, $\rho \approx 1.1$ g mL^{-1}, $M_w \approx 20\,000$ g mol^{-1}, $T_{melt} \approx 65\ °C$) and silica particles (#SS1205, Industrial Powders) constitute the ternary experimental system. The particles are spherical with an average diameter of 2 μm and a monomodal size distribution. The particles were made hydrophobic by coating them with dichlorodimethylsilane (DCDMS) as follows: a ~100 mL container, quarter-filled with particles was tumbled at a few RPM. Nitrogen was bubbled through a DCDMS to remove any droplets/mist, and the DCDMS-saturated nitrogen was then passed through the tumbling container for 1 hour. SEM (shown later in Fig. 1) confirms that DCDMS-modified particles, when added to a PEO/PIB blend, are partially-wetted by both phases. This contrasts with the unmodified particles that when added to a PEO/PIB blend, are fully-wetted by PEO.

2.2 Sample preparation

Similar to our previous research, a temperature-controlled custom ball mixer was used to mix all three components. A two-step procedure was followed: PEO and PIB were first blended in the desired ratio at 600 RPM at 80 °C for 2 minutes. Then, particles were added to the mixing cup and the three components were blended for an additional 5 minutes. This blending procedure is similar to that used in our previous research except for some minor modifications (higher speed during blending, and mechanical redesign of how the mixer is held closed during blending). The mixed sample was quenched by cooling to roughly 5 °C to ensure complete crystallization of the PEO.

Sample stubs were prepared for SEM characterization. As previously, we exploit the fact that n-octane can selectively dissolve the PIB while leaving the PEO completely unaffected. For samples with PIB as the continuous phase, a small quantity of sample was first transferred into a vial filled with n-octane, and held overnight to dissolve the PIB matrix. The residual sediment (a composite structure comprising particles and PEO) was then collected, transferred onto a filter (Millipore, 0.1 μm pore size) stuck onto a carbon-taped SEM stub, and rinsed with octane several times. For samples with PEO as the continuous phase, a small portion of sample was first cooled and fractured in liquid nitrogen. The fractured surface was then washed several times with n-octane before placing on the stub. All SEM stubs were then left to dry, and coated with an Au/Pd sputtering target (Cressington) for 90 seconds at 40 mA before sent into the SEM chamber.

In addition to scanning electron microscopy, a limited amount of optical microscopy was also conducted on both, molten and quenched blends. All the information from these images are completely consistent with SEM images, but particles are not clearly visible. Hence optical images are not discussed here.

3. Results

Before turning to particle effects, we will briefly summarize the morphology of the PEO/PIB blends in the absence of particles. Consistent with our previous research,[14] we find that blends of PEO and PIB show simple droplet-matrix morphologies, either PEO drops in a PIB continuous phase (at high PIB content) or PIB drops in a PEO continuous phase (at high PEO content). Phase inversion was reported at about 60% PEO. The drop size was found to increase as phase inversion composition was approached from either size. Unlike in many polymer blends, we did not find any composition region of co-continuity, nor any fibrillar morphologies near phase inversion. This is likely due to the fact that the viscosity of our polymers is two to three orders of magnitude lower than of typical molten plastics, and hence any complex microstructure that may be present during mixing rapidly breaks into a droplet-matrix structure as soon as mixing ceases.
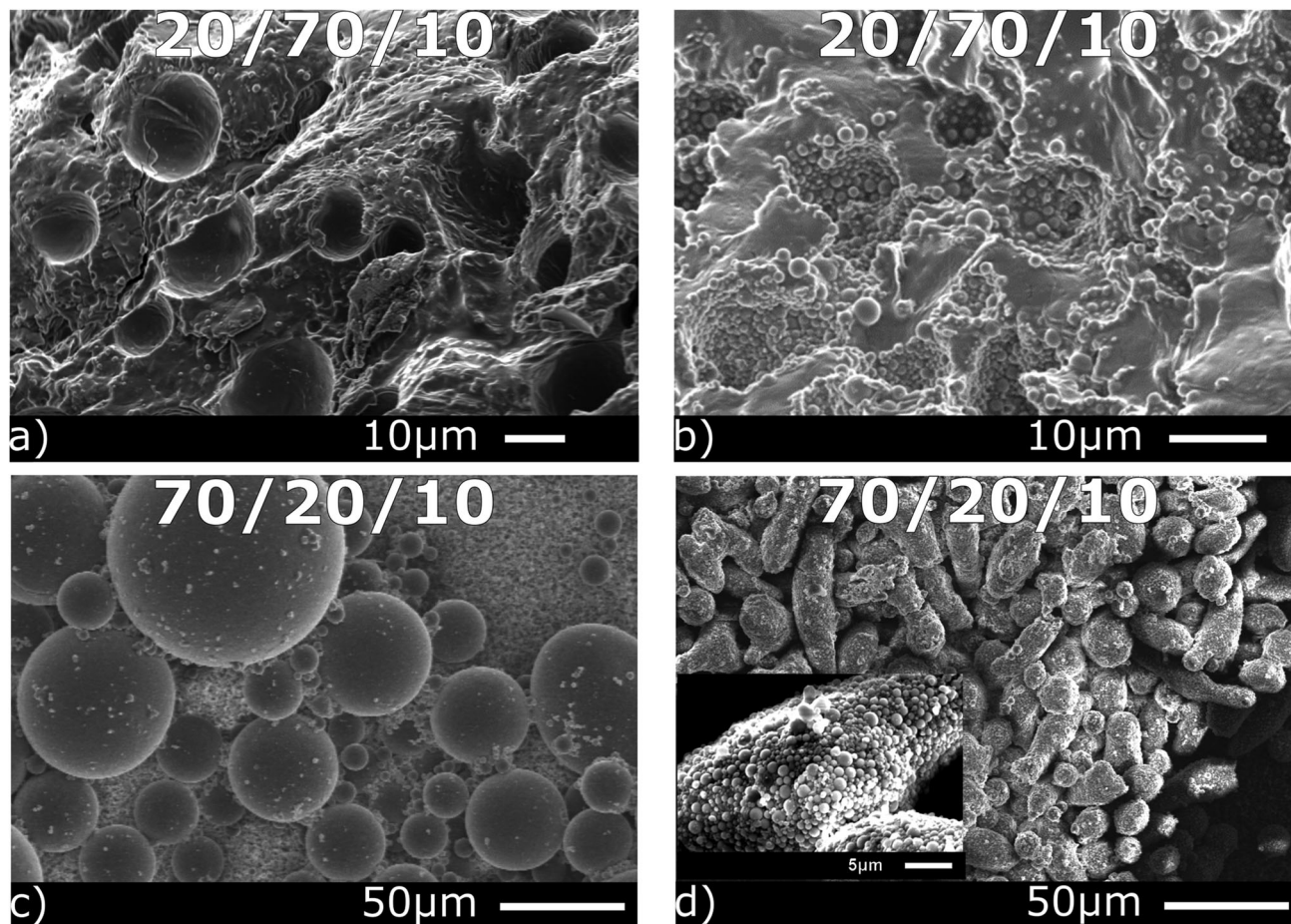
Fig. 1   SEM images comparing blends with unmodified silica particles (a and c) *vs.* blends with DCDMS–modified silica particles (b and d). The inset of (d) shows a higher magnification for the same blend to show the particles crowded at the interface. The numbers at the top of each image are the blend composition in the format of PIB/PEO/particle volume ratio.

The rest of this Section 3 deals with the effects of particles on the morphology. A total of 26 blends were examined, and representative SEM images are shown in ESI,† Fig. S2. Due to the large number of samples, it is difficult to gauge the wide-ranging effects of particles all at once. Accordingly, the following sections present the results in a more piece-wise fashion proceeding from dilute to concentrated particle loadings. The experimental results for particle effects are organized as follows. In Section 3.1 we first show that the DCDMS modification is successful in changing the particles from being fully-wettable by PEO to being partially-wetted by both phases. This is followed by four sections that discuss changes in drop size due to particles (Section 3.2), changes in morphology at low particle loading (Section 3.3), and changes in phase continuity due to higher particle loadings (Section 3.4) and particle wettability (Section 3.5).

3.1   Validation of surface modification

As mentioned in the Introduction, the purpose of this research was to construct a morphological map of ternary blends with partially-wettable particles, and compare with the case (Fig. S1, ESI†) of fully-wettable particles examined previously.[5] Thus it is

first critical to verify that the DCDMS treatment actually modifies the surface wettability towards PEO and PIB. This was tested (Fig. 1) by comparing the morphology of four particle-containing blends, two with 10% DCDMS-modified silica particles, and two with 10% unmodified silica particles. The blend compositions were selected so that in two cases PEO was in a large majority (70%) and hence PEO became the continuous phase, whereas in the other two cases, PIB was in a large majority (70%) and hence PIB became the continuous phase. Fig. 1a and b shows the fracture surface of the two blends with PEO as the continuous phase after extraction of the PIB, leaving behind craters. The inner surface of the craters appears smooth for the sample containing unmodified particles (Fig. 1a). In contrast, in Fig. 1b, the crater surfaces are covered with DCDMS-modified particles. Fig. 1c and d show the two blends with PIB as the continuous phase. In this case, upon extraction of the PIB, the dispersed phase (comprising the PEO and silica) is recovered for imaging. The dispersed phase of the blend with the unmodified particles (Fig. 1c) appears smooth indicating that the particles are inside the PEO drops. In contrast, the dispersed phase of the blend with the DCDMS-modified particles is heavily covered with particles suggesting that the particles are partially-wetted by

PEO and PIB (Fig. 1d). Based on these images, the DCDMS surface modification process is deemed to be successful in creating partially-wettable particles, and therefore suitable for constructing a morphology-composition map for a ternary liquid/liquid/particle mixture with partially-wettable particles.

The images also allow some judgement of contact angles of the DCDMS-coated silica. Due to the polydispersity of the particles and also because the PEO/PIB interface is not flat (indeed not even very smooth), it is difficult to judge a contact angle quantitatively. Nevertheless, judging by the visual appearance of the particles (and in particular, how far the particles protrude out of the PEO phase), the particles appear to be at a near 90° contact angle in Fig. 1d. In Fig. 1b however, the particles protrude less out of the PEO phase suggesting a contact angle of less than 90° as measured through the PEO phase. This comparison of Fig. 1b and d suggests some level of contact angle hysteresis, which may be attributable to the following reason: the blends are prepared by first blending the PEO and PIB in the appropriate proportions, and then adding particles. Thus the particles first encounter (and hence are wetted by) that phase which is continuous prior to particle addition. Accordingly, particles encounter PIB first for Fig. 1d, and PEO first for Fig. 1b. Evidently this initially-wetting phase

affects the final contact angle. Similar contact angle hysteresis can be found in small molecule systems.[28] Furthermore, Fig. 1d results in a near-symmetric wetting, and Fig. 1b results in a preferential wetting by PEO. We never observe preferential wetting by PIB, suggesting that the particles are somewhat PEO-philic, and not neutrally-wetting.

Two other features are noteworthy from Fig. 1. The first is that in both Fig. 1b and d, the dispersed phase is non-spherical in notable contrast to the fully-wetting blends (Fig. 1a and c). Such non-spherical dispersed phases are well-known in Pickering emulsions, and indeed were noted even in an early description of Pickering emulsions.[17] The second is that the dispersed phase is much larger when PEO is the dispersed phase than when PIB is the dispersed phase. We will discuss both points later in the paper.

3.2 Dilute particle loading: increase in size of the dispersed phase

To test particle effects at dilute loadings, experiments were conducted on blends with just 1% particles. Even at this low loading, particles sharply increase drop size as illustrated in Fig. 2. At a PIB:PEO ratio of 80:20, PIB forms the continuous phase, and the PEO drops are fairly uniform-sized and round
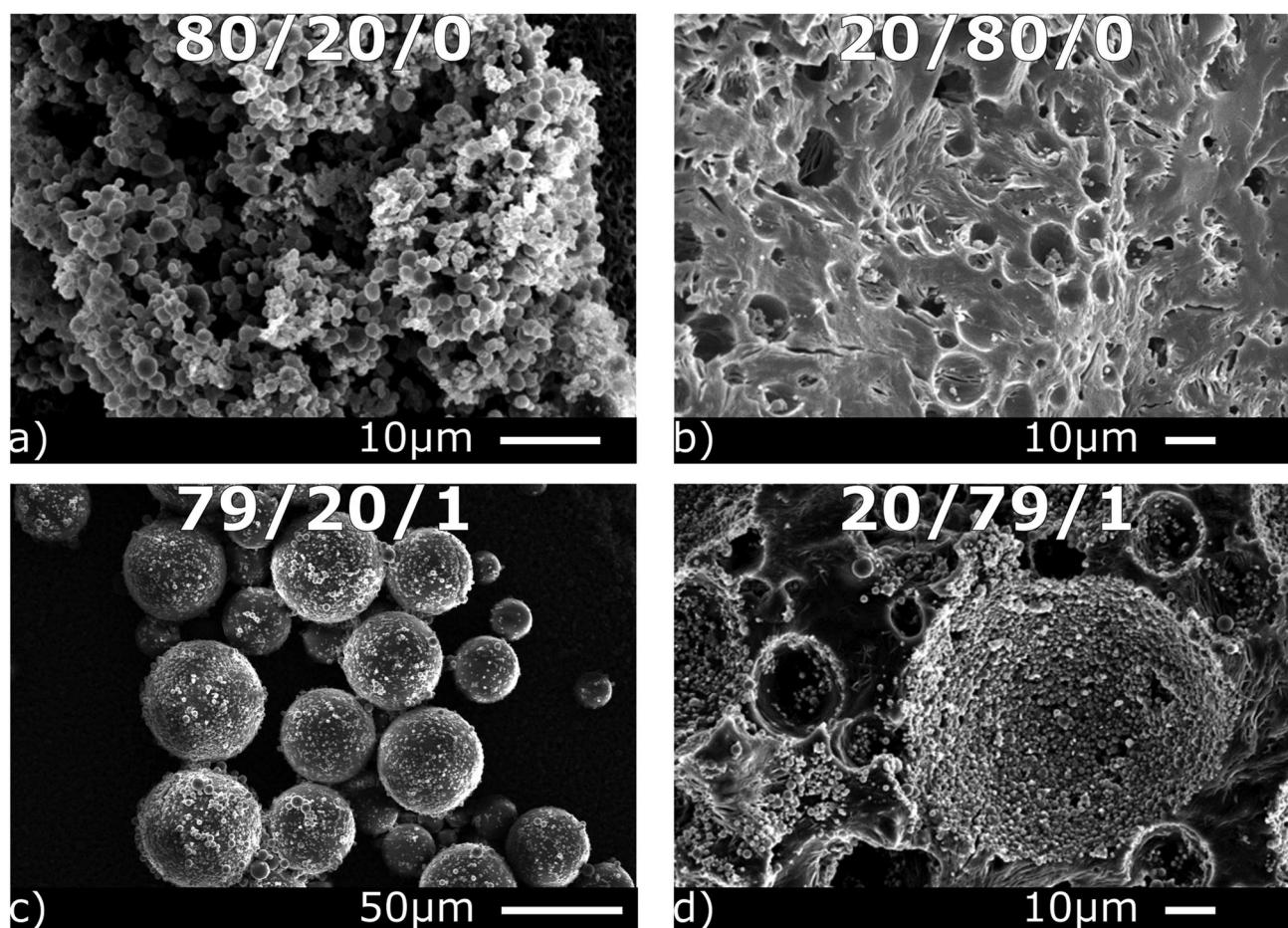

Fig. 2 SEM images of the effect of adding 1% DCDMS–coated particles on blends with PIB as the continuous phase (a and c) and PEO as continuous phase (b and d). The PIB/PEO/particle volume ratios are noted in each image.

with a typical diameter of 2 μm (Fig. 2a). Addition of 1% particles induces a massive increase in the PEO drop size to 20 μm (Fig. 2c). Fig. 2b shows the reverse situation: at a PIB : PEO ratio of 20 : 80, PEO forms the continuous phase, and in the absence of particles, the PIB drop size is several microns. Upon addition of 1% particles, the drop size increases by several fold. Such particle-induced increase in drop size has been noted previously in our research[11,29] (indeed at even lower particle loading). We attribute this to an increase in coalescence rate due to particles by a mechanism analogous to the "bridging–dewetting" mechanism well-known in in aqueous systems, although as originally proposed, the bridging–dewetting mechanism applies only when the particles are preferentially-wetted by the drop phase.[29–31]

Fig. 2 also shows another unexpected feature: even in the absence of particles, there is a large difference in the dispersed phase size: the PEO drops in Fig. 2a are far smaller than the PIB drops in Fig. 2c. This large size difference appears even though both these blends have the same dispersed phase loading, and even though their viscosity mismatch is only modest. The cause of this asymmetric behavior of the particle-free blends is not clear. Nevertheless, similar asymmetric behavior has been noted previously in other blends of immiscible polymers.[32] We will not discuss this drop size asymmetry in particle-free mixtures further in this article.

3.3 Morphological changes with composition at 10% particles

We now turn a higher particle loading of 10%, which is already higher than used in much of the past literature on oil/water Pickering emulsions or particle-filled polymer blends. Nine blends with various PIB : PEO volumetric ratios ranging from 87 : 3 to 3 : 87 were examined, all at 10% particles (Fig. S2, ESI†). Six of these have been selected in Fig. 3 to illustrate the

morphological changes with composition. The magnifications are selected to match the appropriate length-scale of each sample, and we will discuss each in turn.

In Fig. 3a, at 3% PEO, the particles appear to be aggregated together by PEO, which resembles the "pendular/funicular" morphology obtained previously for fully-wetting particles. At even lower PEO loading (the composition of 89/1/10 in volume in Fig. S2, ESI†), many of the particles appear to be bonded to each other pairwise (i.e. pendular menisci), whereas in Fig. 3a, multiple particles are bonded by a single "funicular" meniscus. It is noteworthy that of all the morphologies in Fig. 3, this is the only one that also exists in the fully-wetting case studied previously. All the other morphologies in Fig. 3 are altogether different from those seen in Fig. S1 (ESI†).

Upon increasing the PEO content to 20% (Fig. 3b) the morphology changes drastically: the dispersed phase PEO now adopts irregular elongated shapes of several tens of microns in size. With a further increase in the PEO loading, the size scale of the dispersed phase increases, e.g. compare Fig. 3b, Fig. S2h (ESI†) and Fig. 3c, respectively at 20, 30 and 36% PEO. Along with the increase in drop size, the interface becomes much more smooth, higher magnification images at these compositions all show that the surface of such dispersed phases is tightly covered with particles. An example is shown in the inset to Fig. 3c.

With a further increase in PEO fraction, phase inversion occurs. At 45% PEO (Fig. 3d), the morphology qualitatively resembles an inverted version of Fig. 3c: an irregularly-shaped dispersed phase that is coated with particles. Similarly, Fig. 3e comprises particle-covered PIB drops, which is an inverted version of Fig. 3b, albeit with a much smaller size scale. Finally, at the lowest PIB loading, Fig. 3f, the sample still consists of PIB drops, but now the drop size is comparable to that of the particles.
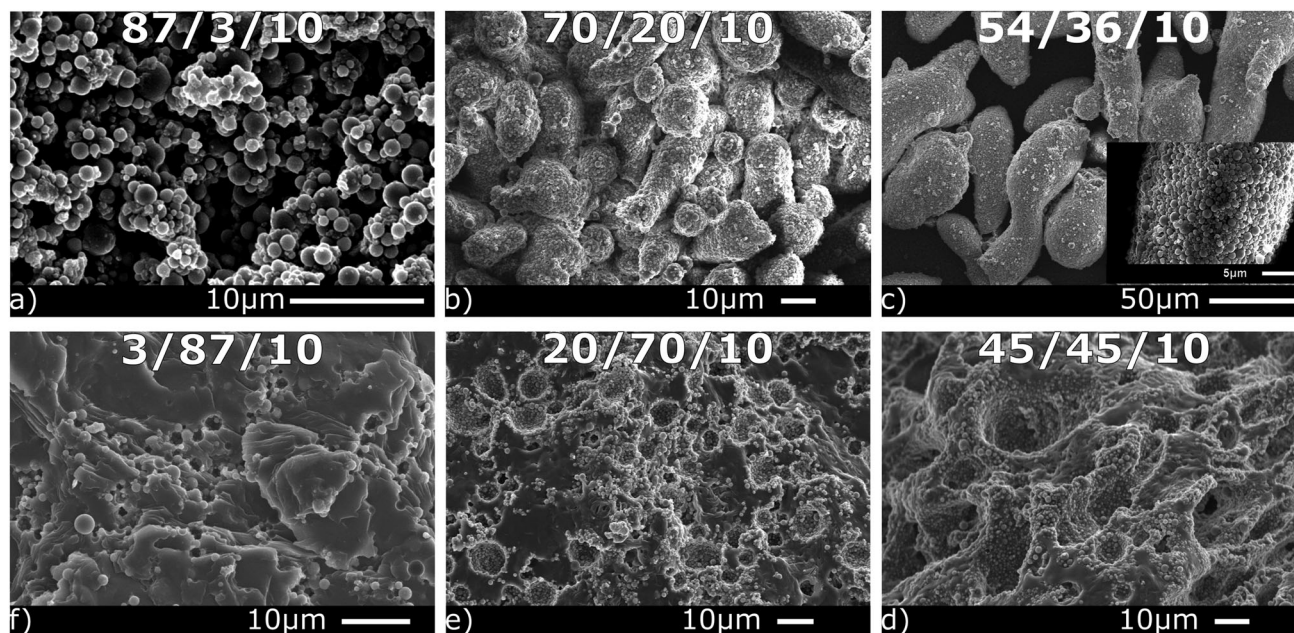

Fig. 3 Ternary blend morphology at various PIB/PEO/particle ratios listed in each image. The particle loading is 10% in all cases.

3.4 High particle loadings and co-continuous morphologies

We now turn to a much higher particle loading of 20% and 30%, values far higher than used in most of the existing literature on Pickering emulsions or on filled polymer blends. A total of nine blends were prepared at these two loadings (Fig. S2, ESI†). The morphological trends were found remain broadly similar to those at 10% but with some differences. One difference is the sharp decrease in the lengthscale of the dispersed phases as particle loading increases. The second is the appearance of highly branched morphologies that appear, at least visually, to be co-continuous. Various methods including image analysis, solvent extraction, electrical conductivity measurements and rheological measurement have been considered for judging the phase continuity of polymer blends.[33] Here however, well-established quantitative methods of judging phase continuity, which typically involve blends of solid samples, are difficult to apply since PIB is a liquid. Instead, we rely on qualitative visual judgment.

To illustrate these two trends, the morphologies at selected compositions are shown in Fig. 4. The compositions of Fig. 4 were selected such that the middle column (Fig. 4b and e) correspond to morphologies that appear (at least visually) to be co-continuous. The left and right columns correspond respectively to the blends with somewhat lower and somewhat higher PEO content respectively.

At 10% particles, co-continuous morphologies are not evident, and hence only dispersed phase morphologies are shown (Fig. 4g and h). As the particle loading reaches 20%, the branched PEO structures are found to join together into the morphology of Fig. 4e which appears co-continuous (indeed it remains intact when the PIB is dissolved). With further increase in particle loading, the lengthscale of the morphology reduces further (Fig. 4b). The inset to Fig. 4b shows a higher resolution SEM of the fractured surface which reveals that the PEO-phase itself contains a smaller-scale microstructure that incorporates both the particles and the PEO. This latter point will be discussed further below.

On the PIB-rich side of phase inversion (left column of Fig. 4), at 10% particles, the 54/36/10 blend (Fig. 4g) shows a branched dispersed phase, which may be regarded as a
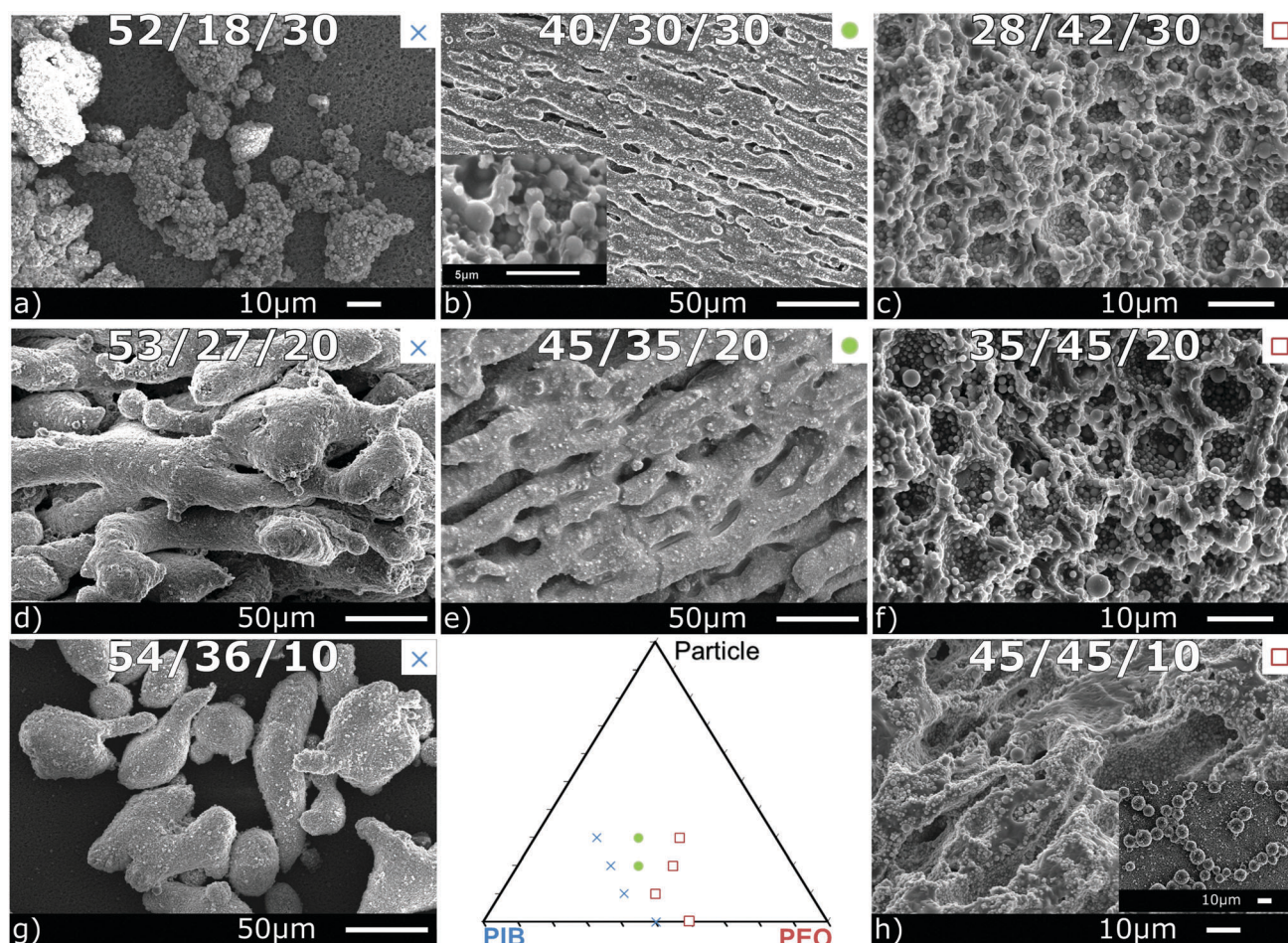

Fig. 4 Morphologies near phase inversion at various particle loadings. The PIB/PEO/silica ratios are listed in each image. Left column are PIB-continuous, right column are PEO-continuous, and mid column are co-continuous. The inset in (b) shows a magnified image of structure inside the percolating branches. The inset in (h) shows the PEO dispersed phase using OTS-modified silica particles at same composition. The top right of each image shows the symbol used in the triangle for each type of phase continuity.

precursor to a truly co-continuous morphology. With increase in particle loading to 20% (Fig. 4d), the branching increases, and the 53/27/20 sample is nearly co-continuous (upon extracting the PIB, the sample fragmented to some degree). At 30% particle loading however (Fig. 4a), the morphology looks distinctly different: it is no longer highly branched, and the surface appears highly irregular. Indeed this visually resembles a capillary aggregate morphology seen in mixtures with fully-wetting particles[13] although in the present case, the particles are not fully-wetting and capillary aggregates are unlikely to form. The likely reason for this morphology is that the particle loading now exceeds the dispersed phase loading. Since the particles have a strong preference to stay at the interface, a highly irregular interface, by offering a larger interfacial area, may be able to accommodate more particles at the interface.

On the PEO-continuous side (the right column in Fig. 4), the dispersed phase (now PIB) appears interfacially-jammed. This is somewhat analogous to the left column in Fig. 4, but with two differences. First, highly elongated and branched dispersed phases do not appear when PIB is the dispersed phase (compare for instance Fig. 4d and f). Second, consistent with the previous section, the size-scale of the morphology is much smaller when the dispersed phase is PIB *vs.* when the dispersed phase is PEO.

Finally, it is noteworthy that the phase inversion composition shifts significantly due to particles. In the discussion below, we will present a morphological map of this ternary system, and the corresponding Fig. 6 shows that particles increase the PIB : PEO ratio at phase inversion, *i.e.* particles help maintain PEO phase continuity even when the PEO loading reduces.

3.5 Effect of particle wettability on ternary blend phase inversion composition

The previous Section 3.4 concluded that the DCDMS-modified silica particles, which are partially-wetting towards both phases, shift the phase inversion point towards higher PIB : PEO ratio. In fact our previous research on the unmodified silica particles (which are fully-wetted by PEO) showed a similar shift.[14,16] The fact these two particle types with very different wettability have a similar effect (increase the PIB : PEO ratio at phase inversion) raises the following question: does the shift in phase inversion composition depend on particle wettability at all? Or is there some inherent asymmetry in the PEO and PIB fluids themselves that tends to favor PEO-phase continuity regardless of the nature of particles added?

To address this question, a limited number of blends were prepared using the same silica particles, but modified with a different silane, octadecyltrichlorosilane (OTS). Since OTS has a long alkyl chain, it makes the particles much more hydrophobic, and hence much more PIB-philic, than DCDMS-modified particles.[11] Two blend compositions, PIB/PEO/silica = 45/45/10, and 36/54/10 were prepared, and the corresponding morphologies are shown in Fig. 5. In the 45/45/10 blend (PIB : PEO = 1 : 1) PEO forms the dispersed phase, and particles protrude far out of the PEO drops (Fig. 5a) confirming that they are more PIB-philic than the DCDMS-modified particles. Indeed the particles
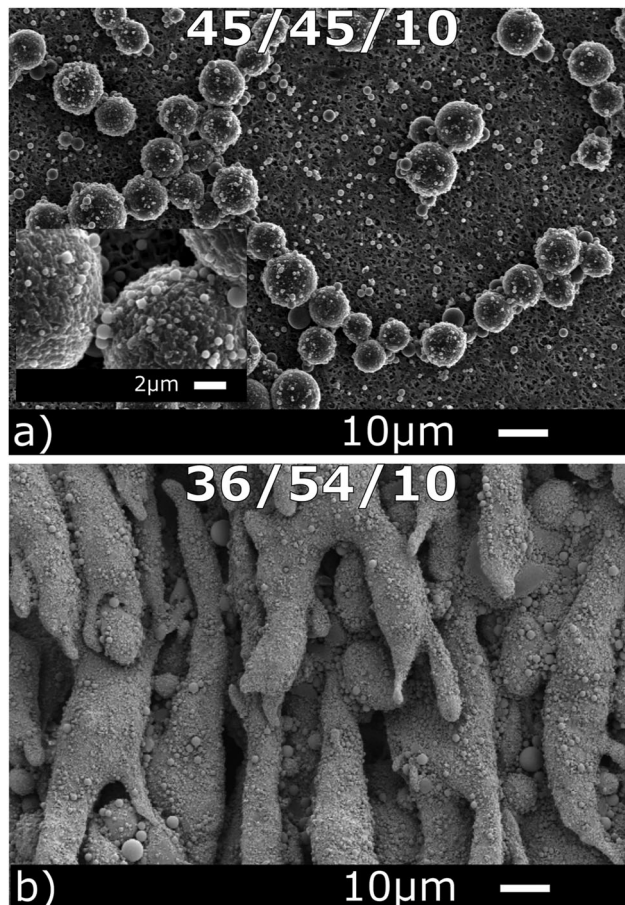

Fig. 5 Testing phase continuity of polymer blends containing OTS-modified silica particle at the two compositions (in the format PIB/PEO/silica) indicated in each image.

protrude sufficiently far that they can bridge together PEO drops as shown in the inset to Fig. 5a. Such bridging was already seen previously, albeit with monodisperse OTS-silica particles at much lower loading.[11,30] In the 36/54/10 blend (PIB : PEO = 2 : 3) an elongated or co-continuous morphology appears (Fig. 5b). We may then summarize the phase continuity results in Table 1. It is immediately obvious that at certain PIB : PEO ratios, the phase continuity does depend on the particle type. Most importantly, at the 1 : 1 PIB : PEO ratio, the phase continuity of the blends with OTS-modified particles is "flipped" as compared to the unmodified or the DCDMS-modified particles. We therefore conclude that the changes in phase continuity does depend on the wettability of the particles. Specifically, addition of particles favors continuity of the phase that is preferentially-wetted by the particles, as has also been observed in oil/water Pickering emulsions.[28,34–37]

4. Discussion

4.1 State map and phase inversion

A major goal of this paper was to construct a state map of the microstructure as a function of composition and contrast it with the previously-constructed map for fully-wettable particles.

Table 1 Volume ratio of phases near phase inversion

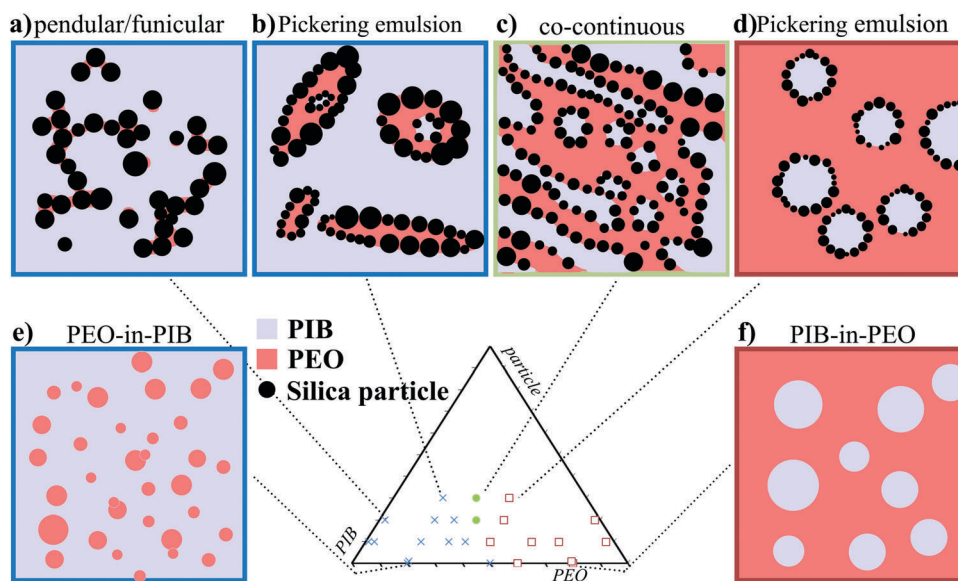|	Approx. PIB : PEO ratio of samples bracketing phase inversion		
Particles	3 : 2	1 : 1	2 : 3
None Unmodified[14]	PIB-cont. (Fig. S1, ESI)	PIB-cont. (Fig. S2b, ESI) PEO-cont. (Fig. S1, ESI)	PEO-cont. (Fig. S2c, ESI)
DCDMS-modified (10%)	PIB-cont. (Fig. 3c)	PEO-cont. (Fig. 3d)	
OTS-modified (10%)		PIB-cont. (Fig. 5a)	Co-cont. (Fig. 5b)

Fig. 6 A summary of all the composition studied and different morphology sketches at various compositions. From left to right: (a) pendular/funicular state when PEO is the minority phase; (b) PEO-in-PIB Pickering emulsion; (c) co-continuous state; (d) PIB-in-PEO Pickering emulsion; (e) PEO-in-PIB suspension; (f) PIB-in-PEO suspension.

The morphological observations of Section 3 suggest the morphological state map of Fig. 6, where the various morphologies are shown in schematic form. Pendular/funicular structures appear when PIB is the continuous phase and the volume fraction of PEO (ϕ_{PEO}) is less than that of particles (ϕ_p) PEO-in-PIB Pickering emulsion microstructures appear when $\phi_p < \phi_{PEO}$. On the PEO-continuous side, PIB-in-PEO Pickering emulsions occur at all particle loadings, including when volume fraction of PIB (ϕ_{PIB}) is less than that of particles (ϕ_p). In this latter situation, since the particle loading exceeds the PIB drop loading, there must be numerous particles that are not covering the visible PIB drops. We infer that there may be a population of very small PIB-bound particle aggregates dispersed in the PEO phase which are not readily identifiable by our SEM imaging method. The two Pickering emulsion states are separated by a co-continuous morphology, and Fig. 5b shows that such a co-continuous state appears even with particles of a very different wettability. To our knowledge, such co-continuous morphologies have never been reported in small-molecule oil/water systems prepared by mixing (co-continuous bijels can be prepared as an arrested state after spinodal decomposition, but not by blending particles into a two-phase oil/water mixture[8,38]). We believe that the much lower viscosity of oil/water systems is responsible for this: any

complex morphology that may exist under flow conditions rapidly reverts to a conventional spherical-drop morphology immediately after mixing stops.

There are sharp differences compared with the state map for fully-wetting particles.[14] The pendular/funicular microstructure of particles bound by PEO is the only one that appears with both unmodified silica (Fig. S1, ESI†) and with the DCDMS-coated silicas (Fig. 6). Another feature in common with Fig. S1 (ESI†) is that particles stabilize co-continuous morphologies, whereas in the particle-free blends, co-continuous morphologies do not appear. However the microstructural details of the co-continuity are altogether different: the co-continuity in Fig. S1 (ESI†) is due to internal jamming of the PEO phase, whereas those in Fig. 4e and 5b are likely attributable to interfacial jamming of particles as well as the particle-covered drops within the PEO phase (see below). In the very apt description of Spicer *et al.*,[39,40] the former is endo-skeletal jamming, whereas the latter is exoskeletal. Finally, partially-wetted particles greatly affect the morphology across all compositions including low and high particle loadings, and across the entire range of PIB : PEO ratios. In contrast, fully-wetted particles affected the morphology significantly only when ϕ_p exceeded or was comparable to the wetting phase loading, ϕ_{PEO}.[14,16]

The morphological map of Fig. 6 is notably asymmetric. The asymmetries include the following:

(1) Pendular/funicular microstructures appear unambiguously only when PEO is the dispersed phase. However we acknowledge that it is difficult to make a firm judgement about morphologies such as Fig. 3f. On one hand, the appearance of PIB craters suggests a Pickering emulsion of PIB drops surrounded by PEO. On the other hand, the drops may also be bonded to each other, similar to particle network dubbed "capillary state suspension" by Koos et al.[4]

(2) For the Pickering emulsion microstructures, the dispersed phase has a larger size when PEO is the dispersed phase as compared to when PIB is the dispersed phase.

(3) Near phase inversion, the PEO phase is itself a Pickering emulsion, i.e. the PEO phase contains particle-covered PIB drops.

(4) Addition of particles shifts the phase inversion composition "leftwards" on the composition diagram, i.e. in the presence of particles, the PEO can retain continuity at a higher PIB : PEO ratio than in the absence of particles. Analogously, at $\phi_p \geq 0.2$ where co-continuous morphologies appear, the PIB : PEO ratio for the co-continuous morphologies exceeds 1 : 1.

The latter three trends all seem to be attributable to preferential wettability of the PEO towards the particles. More specifically, the Pickering emulsion literature suggests that an emulsion is highly stable against coalescence if the continuous phase is preferentially-wetted by the particles, but much less stable if the dispersed phase is preferentially-wetted by the particles.[41] Such differential stability would immediately explain item 2 above, i.e. the PIB drops are small because PEO wets the particles preferentially making the PIB-in-PEO emulsion very stable. Moreover, if the PIB-in-PEO Pickering emulsion is highly stable, but ϕ_{PEO} is too small to ensure PEO phase continuity, it is easy to envision the stable emulsion itself becoming dispersed into PIB (item 3 above). Finally, item 4 above may be attributable to two related causes: faster coalescence of PEO drops implies that continuity of the PEO phase is favored,[42] and furthermore, the PEO phase tends to incorporate significant amounts particle-coated PIB drops near phase inversion. Thus, the volume fraction of the PEO phase is effectively "expanded", making it easier for that phase to become continuous.

4.2 Interfacial jamming

In the oil/water Pickering emulsion literature, it has been long-recognized that particles can crowd at the interface and give rise to non-spherical drop shapes, a phenomenon generally called interfacial jamming.[7,43] Similar phenomena have been noted in air/water systems, and the corresponding jammed dispersed phases are often called particle-covered bubbles or liquid marbles.[44,45] Furthermore, the same idea of interfacial jamming can be exploited to stabilize co-continuous morphologies.[8,46] Interfacially-jammed morphologies readily appear in our systems at a variety of compositions (Fig. 6), and we will discuss them here.

Interfacial jamming appears because particles adsorb at liquid–liquid interfaces very strongly, with the adsorption energy typically being several orders of magnitude higher than

kT.[41,47] As a result, the desorption of individual particles from the interface is unlikely. Moreover, since the particles have homogeneous surfaces (i.e. are not patchy), unlike surfactants, they cannot form micelles. Thus crowding particles at the interface leads to interfacial jamming.

Accordingly, the simplest "morphological model" is that interfacial jamming occurs when the liquid–liquid interfacial area is exactly what is needed to accommodate all the particles at the interface. The corresponding area per unit volume (i.e. the cross sectional area of the particles per unit volume) can be estimated as ϕ_p/D_p where D_p is the diameter of the particles. Consider now an emulsion-type morphology (with either PEO or PIB as the dispersed phase) with L being lengthscale of the morphology. For example, L may be regarded approximately as a mean drop size (if the dispersed phase is in the form of round drops), or a mean cylinder size (if the dispersed phase is roughly cylindrical). The interfacial area per unit volume of the morphology is therefore roughly ϕ_{disp}/L where ϕ_{disp} is the volume fraction of the dispersed phase. If the morphology is on the verge of jamming, we can equate the above two areas per unit volume to obtain $L^* = D_p \dfrac{\phi_{disp}}{\phi_p}$. This L^* is the largest possible lengthscale for the dispersed phase if all the particles reside at the interface; specifically, if $L < L^*$ (e.g. under intense mixing conditions), then interfacial jamming cannot happen and hence the dispersed phase will remain spherical. On the other hand if the flow is relatively weak, the dispersed phase will coarsen, but become no bigger than L^*. We acknowledge that this model does not predict a value for average droplets size of the dispersed phase, which is determined by the volume fraction of the dispersed phase, the rate of coalescence of the dispersed phase, and flow strength. This model only predicts the largest size the dispersed phase can have, which is also the sizescale below which the dispersed phase must be unjammed and hence spherical. This model is based on assumption that the particles are monodisperse, whereas in reality, the smallest particles are most effective in covering interfaces. Nevertheless, L^* provides a first order estimate of the largest sizescale of the microstructure that can avoid jamming.

Of all the samples examined, Fig. 2c is the only morphology that is not jammed, i.e. has unambiguously spherical drops whose interface is not crowded with particles. Indeed, for this sample $L^* = 20D_p = 40$ μm is predicted, whereas most drops are comparable or smaller in diameter. This is consistent with the idea that if $L < L^*$, interfacial jamming will not happen. For most samples with PIB as the dispersed phase, the L^* is found to be close to the morphological lengthscale estimated from SEM images. For instance, for Fig. 4f, $L^* = 1.75D_p = 3.5$ μm is calculated, and a majority of PIB drops appear to have a diameter near 10 μm. In contrast, for the samples with PEO as the dispersed phase, the calculated values of L^* underestimate the morphological sizescale. For instance, for Fig. 4d $L^* = 1.35D_p = 2.7$ μm is calculated whereas the interfacially-jammed dispersed phase has a typical width of a few tens of microns.

For these PEO-dispersed phase samples, the fact that $L \gg L^*$ suggests that at least one of the assumptions underlying the

calculation of L^* must be incorrect. For instance, if some of the particles stay dispersed into one of the bulk phases (*i.e.* behave similar to fully-wetted particles), the basic assumption that the all the particles are interfacially-adsorbed is violated. In fact, the Section 4.1 and the inset to Fig. 4b support a different view, that the morphology is more "topologically" complex than a simple emulsion. Specifically, the PEO phase is itself a Pickering emulsion which incorporates particles.

The central conclusion therefore is that in such ternary particle/liquid/liquid systems, co-continuous morphologies cannot be readily tuned by changing particle loading. For instance, in the bijel literature, the lengthscale of the co-continuous structures was found to be proportional to the reciprocal of the particle loading.[8,38] This was based on the same picture of interfacial jamming as above (indeed above we also calculated $L^* \propto \dfrac{1}{\phi_p}$). However in the co-continuous morphologies developed by blending, such simple tuning of lengthscales may not be possible; the system "decides" whether particles should be located at the interface of the co-continuous structure or on drops within one of the phases. Indeed other microstructures may be possible under some conditions, *e.g.* a co-continuous morphology in which one of the phases is a pendular network.

5. Conclusion

To summarize, we have conducted a comprehensive morphology-composition mapping of a ternary mixture composed of two molten immiscible polymers (polyisobutylene and polyethylene oxide) and spherical silica particles which are partially-wetted by both polymer phases. To our knowledge, this study, similar to our previous study of the fully-wetting case, encompasses the widest composition range examined for a single ternary liquid/liquid/particle system. The partially-wettable particles significantly affect the morphology across the entire range of compositions. The various morphologies observed include pendular/funicular aggregates of particles, Pickering emulsions, co-continuous morphologies, and (when the particle strongly prefer one fluid) particle-bridged Pickering emulsions. The particles induce coalescence of the dispersed phase at dilute particle loading, create interfacially-jammed Pickering emulsions, and stabilize interfacially-jammed co-continuous morphologies. At least one of the morphologies appears to be topologically-complex: a co-continuous morphology where one phase is a Pickering emulsion. This suggests that such ternary blends may adopt microstructures that are difficult to predict based on simple considerations of wettability and composition.

Many of the particle effects are asymmetric, *i.e.* the morphology is sharply different depending on which fluid is the continuous phase. The asymmetries are likely attributable to the modest preference of the particles towards one of the phases, polyethylene oxide. Most importantly, the particles shift the phase inversion composition such that polyethylene oxide, the phase that preferentially-wets the particles, tends to become the continuous phase.

In combination with the previous research on the fully-wetting case, this research represents the most detailed morphological

mapping of a ternary liquid/fluid/particle mixture in the parameter space defined by the composition and the wettability of the particles. It would be interesting to see if other systems with different chemistry and particle sizes show similar morphologies at similar composition and particle wettings. If so, they would confirm the idea[2] that diverse ternary systems share a somewhat universal microstructural map.

Conflicts of interest

There are no conflicts to declare.

Acknowledgements

References

1 E. Koos, *Curr. Opin. Colloid Interface Sci.*, 2014, **19**, 575–584.
2 S. S. Velankar, *Soft Matter*, 2015, **11**, 8393–8403.
3 J. McCulfor, P. Himes and M. R. Anklam, *AlChE J.*, 2011, **57**, 2334–2340.
4 E. Koos and N. Willenbacher, *Science*, 2011, **331**, 897–900.
5 T. Domenech and S. S. Velankar, *Soft Matter*, 2015, **11**, 1500–1516.
6 J. Zhang, H. Zhao, W. Li, M. Xu and H. Liu, *Sci. Rep.*, 2015, **5**, 16058.
7 R. Aveyard, B. P. Binks and J. H. Clint, *Adv. Colloid Interface Sci.*, 2003, **100**, 503–546.
8 E. M. Herzig, K. A. White, A. B. Schofield, W. C. K. Poon and P. S. Clegg, *Nat. Mater.*, 2007, **6**, 966–971.
9 M. E. Cates and P. S. Clegg, *Soft Matter*, 2008, **4**, 2132–2138.
10 M. N. Lee, H. K. Chan and A. Mohraz, *Langmuir*, 2012, **28**, 3085–3091.
11 S. P. Nagarkar and S. S. Velankar, *Soft Matter*, 2012, **8**, 8464–8477.
12 T. Domenech and S. Velankar, *Rheol. Acta*, 2014, **53**, 593–605.
13 T. Domenech, J. Y. Yang, S. Heidlebaugh and S. S. Velankar, *Phys. Chem. Chem. Phys.*, 2016, **18**, 4310–4315.
14 T. Domenech and S. S. Velankar, *J. Rheol.*, 2017, **61**, 363–377.
15 J. Y. Yang and S. S. Velankar, *J. Rheol.*, 2017, **61**, 217–228.
16 D. Amoabeng, D. Roell, K. M. Clouse, B. A. Young and S. S. Velankar, *Polymer*, 2017, **119**, 212–223.
17 S. U. Pickering, *J. Chem. Soc., Trans.*, 1907, **91**, 2001–2021.
18 B. P. Binks, *Curr. Opin. Colloid Interface Sci.*, 2002, **7**, 21–41.
19 T. Ngai, S. A. F. Bon, H. J. Butt, I. Hamley, H. A. Stone, C. Wu, B. J. Park, P. Clegg, S. Biggs and H. Zhao, *Particle-stabilized Emulsions and Colloids: Formation and Applications*, Royal Society of Chemistry, London, 2014.
20 T. S. Horozov and B. P. Binks, *Angew. Chem., Int. Ed.*, 2006, **45**, 773–776.

21 M. N. Lee and A. Mohraz, *Adv. Mater.*, 2010, **22**, 4836–4841.

22 F. Bossler and E. Koos, *Langmuir*, 2016, **32**, 1489–1501.

23 P. Cassagnau, *Polymer*, 2008, **49**, 2183–2196.

24 K. Premphet and P. Horanont, *Polymer*, 2000, **41**, 9283–9290.

25 B. P. Binks, A. J. Johnson and J. A. Rodrigues, *Soft Matter*, 2010, **6**, 126–135.

26 M. Kahlweit and R. Strey, *Angew. Chem., Int. Ed. Engl.*, 1985, **24**, 654–668.

27 H. T. Davis, *Colloids Surf., A*, 1994, **91**, 9–24.

28 B. P. Binks and S. O. Lumsdon, *Phys. Chem. Chem. Phys.*, 2000, **2**, 2959–2967.

29 P. Thareja, K. Moritz and S. S. Velankar, *Rheol. Acta*, 2010, **49**, 285–298.

30 P. Thareja and S. Velankar, *Rheol. Acta*, 2008, **47**, 189–200.

31 P. R. Garrett, *The Science of Defoaming: Theory, Experiment and Applications*, CRC Press, Boca Raton, 2013, pp. 115–308.

32 C. DeLeo, C. A. Pinotti, M. D. Goncalves and S. Velankar, *J. Polym. Environ.*, 2011, **19**, 689–697.

33 J. A. Galloway and C. W. Macosko, *Polym. Eng. Sci.*, 2004, **44**, 714–727.

34 B. P. Binks and S. O. Lumsdon, *Langmuir*, 2000, **16**, 2539–2547.

35 B. P. Binks and S. O. Lumsdon, *Langmuir*, 2000, **16**, 8622–8631.

36 B. P. Binks and S. O. Lumsdon, *Langmuir*, 2000, **16**, 3748–3756.

37 E. S. Read, S. Fujii, J. I. Amalvy, D. P. Randall and S. P. Armes, *Langmuir*, 2004, **20**, 7422–7429.

38 J. A. Witt, D. R. Mumm and A. Mohraz, *Soft Matter*, 2013, **9**, 6773–6780.

39 M. Caggioni, P. T. Spicer, D. L. Blair, S. E. Lindberg and D. A. Weitz, *J. Rheol.*, 2007, **51**, 851–865.

40 A. B. Pawar, M. Caggioni, R. W. Hartel and P. T. Spicer, *Faraday Discuss.*, 2012, **158**, 341–350.

41 B. P. Binks and J. H. Clint, *Langmuir*, 2002, **18**, 1270–1273.

42 J. T. Davies, *Proc. Int. Congr. Surf. Act., 2nd*, 1957, **1**, 426–438.

43 V. Pauchard and T. Roy, *Colloids Surf., A*, 2014, **443**, 410–417.

44 P. Aussillous and D. Quere, *Nature*, 2001, **411**, 924–927.

45 B. P. Binks and R. Murakami, *Nat. Mater.*, 2006, **5**, 865–869.

46 K. Stratford, R. Adhikari, I. Pagonabarraga, J. C. Desplat and M. E. Cates, *Science*, 2005, **309**, 2198–2201.

47 G. Gillies, K. Buscher, M. Preuss, M. Kappl, H. J. Butt and K. Graf, *J. Phys.: Condens. Matter*, 2005, **17**, S445–S464.